AMERICAN SOCIETY FOR MICROBIOLOGY | Journal of Virology®

VIRUS-CELL INTERACTIONS

Autophagy Promotes Replication of Influenza A Virus *In Vitro*

Ruifang Wang,[a,b] Yinxing Zhu,[a,b] Jiachang Zhao,[a,b] Chenwei Ren,[a,b] Peng Li,[a,b] Huanchun Chen,[a,b] Meilin Jin,[a,b] Hongbo Zhou[a,b]

[a]State Key Laboratory of Agricultural Microbiology, College of Veterinary Medicine, Huazhong Agricultural University, Wuhan, China
[b]Key Laboratory of Preventive Veterinary Medicine in Hubei Province, Cooperative Innovation Center for Sustainable Pig Production, Wuhan, China

ABSTRACT Influenza A virus (IAV) infection could induce autophagosome accumulation. However, the impact of the autophagy machinery on IAV infection remains controversial. Here, we showed that induction of cellular autophagy by starvation or rapamycin treatment increases progeny virus production, while disruption of autophagy using a small interfering RNA (siRNA) and pharmacological inhibitor reduces progeny virus production. Further studies revealed that alteration of autophagy significantly affects the early stages of the virus life cycle or viral RNA synthesis. Importantly, we demonstrated that overexpression of both the IAV M2 and NP proteins alone leads to the lipidation of LC3 to LC3-II and a redistribution of LC3 from the cytosol to punctate vesicles indicative of authentic autophagosomes. Intriguingly, both M2 and NP colocalize and interact with LC3 puncta during M2 or NP transfection alone and IAV infection, leading to an increase in viral ribonucleoprotein (vRNP) export and infectious viral particle formation, which indicates that the IAV-host autophagy interaction plays a critical role in regulating IAV replication. We showed that NP and M2 induce the AKT-mTOR-dependent autophagy pathway and an increase in HSP90AA1 expression. Finally, our studies provided evidence that IAV replication needs an autophagy pathway to enhance viral RNA synthesis via the interaction of PB2 and HSP90AA1 by modulating HSP90AA1 expression and the AKT-mTOR signaling pathway in host cells. Collectively, our studies uncover a new mechanism that NP- and M2-mediated autophagy functions in different stages of virus replication in the pathogenicity of influenza A virus.

IMPORTANCE Autophagy impacts the replication cycle of many viruses. However, the role of the autophagy machinery in IAV replication remains unclear. Therefore, we explored the detailed mechanisms utilized by IAV to promote its replication. We demonstrated that IAV NP- and M2-mediated autophagy promotes IAV replication by regulating the AKT-mTOR signaling pathway and HSP90AA1 expression. The interaction of PB2 and HSP90AA1 results in the increase of viral RNA synthesis first; subsequently the binding of NP to LC3 favors vRNP export, and later the interaction of M2 and LC3 leads to an increase in the production of infectious viral particles, thus accelerating viral progeny production. These findings improve our understanding of IAV pathogenicity in host cells.

KEYWORDS HSP90AA1, IAV, LC3, M2, NP, autophagy, replication

Influenza A virus (IAV) is an enveloped virus with a segmented negative-sense RNA genome, causing morbidity and mortality in both humans and animals and threatening their populations with epidemics and pandemics (1, 2). Each RNA segment of IAV is encapsulated by multiple copies of the viral nucleoprotein (NP), which is associated with RNA-dependent RNA polymerase (RdRp) and acts as a key structural determinant of a viral ribonucleoprotein complex (vRNP) (3–6). vRNP is an independent functional unit and critical for catalyzing viral RNA transcription (vRNA-mRNA) and replication (vRNA-cRNA-vRNA) in the nucleus of infected cells (7). RdRp (comprised of PB1, PB2,

Citation Wang R, Zhu Y, Zhao J, Ren C, Li P, Chen H, Jin M, Zhou H. 2019. Autophagy promotes replication of influenza A virus *in vitro*. J Virol 93:e01984-18. https://doi.org/10.1128/JVI.01984-18.

Editor Susana López, Instituto de Biotecnologia/UNAM

Address correspondence to Hongbo Zhou, hbzhou@mail.hzau.edu.cn.

R.W. and Y.Z. have contributed equally to this work.

Received 9 November 2018
Accepted 27 November 2018
Accepted manuscript posted online 12 December 2018
Published 5 February 2019

and PA) is essential for the synthesis of three species of viral RNAs (vRNA, mRNA, and cRNA) (7, 8). The viral RNA synthesis, which is reported to be crucial for virus proliferation and pathogenicity, is dependent on RNP assembly and RdRp activity (8–11). During the early stages of the virus life cycle, virus is first internalized by endocytosis, and then endosomal acidification activates M2 ion channel activity, causing acidification of the virus interior and leading to dissociation of the matrix protein M1 from the vRNP (12). In addition, M2 is also involved in virus assembly, budding, vRNP incorporation, and the production of infectious virions (13–17).

Nutrient deprivation, growth factor depletion, or cellular stress, such as hypoxia, energy depletion, endoplasmic reticulum (ER) stress, high temperature, or high cell density conditions, can activate autophagy (18), one of the major processes for degradation and turnover of long-lived proteins and damaged organelles (19–21). During autophagy, cup-shaped isolation membranes expand to form transient double-membrane sequestering compartments called phagophores, which engulf cytosolic cargo and then fuse with late endosomes for degradation (22, 23). The autophagy-related (ATG) proteins compose several core components of autophagy, which are required for autophagosome formation (24, 25). mTORC1 (mammalian target of rapamycin complex 1) kinase is a key negative regulator of the ULK1 complex (Unc-51-like autophagy activating kinase 1), which is made up of ULK1, ATG101, ATG13, and RB1CC1/FIP200 (26–30) and serves as the initiator in the autophagic cascade. The class III phosphatidylinositol 3-kinase (PI3K) complex (BECN1/Beclin1-ATG14-VPS15-VPS34) and two other conjugation systems, ATG12 (ATG12-ATG5-ATG16) and LC3/ATG8, operate downstream of ULK-1 (31, 32). BECN1, one component of the PI3K complex, not only participates in autophagosome formation but also interacts with different protein complexes regulating the autophagosome-lysosome fusion (33). The ATG12-ATG5 complexes are key regulators that are required to activate autophagy and mediate vesicle elongation during the autophagosome formation process (34). ATG7, a ubiquitin E1-like activating enzyme, is essential for the assembly and function of the LC3 and ATG12 conjugates in the expansion of autophagosomal membranes (35, 36). The ubiquitin-like conjugation reactions are initiated by PI3K complexes, and the activation of PI3K complex results in the recruitment of ATG12-ATG5-ATG16 complex to the isolated membranes and lipidation of LC3-I to generate LC3-II. Membrane association of LC3-II facilitates expansion of the isolation membrane and formation of the autophagosome, and LC3-II stays with the completed autophagosome and is degraded with the inner membrane by lysosomal hydrolysis. LC3 is uniformly distributed, with an acetylated form primarily in the nucleus under conditions without stress, but stress promotes the redistribution of LC3 from the nucleus to the cytoplasm and LC3 punctum formation (37, 38). Thus, a green fluorescent protein (GFP)-tagged LC3 can be used as a specific marker of autophagosomes, and the turnover of lipidated LC3-II can be used to evaluate the autophagy ratio (39).

There is an extremely complex relation between autophagy and invading viruses. Autophagy inhibits pathogenic infection by wrapping viruses in the autophagosome (40, 41), whereas many pathogens exploit autophagy for their replication (42). Several viruses, such as coxsackievirus, dengue virus, and hepatitis C virus, have evolved strategies to use autophagic vesicles for replication (43–47). Furthermore, viruses can regulate the autophagic process to facilitate different stages of the viral replication cycle, ranging from viral entry to egress (42, 48, 49). It is well established that autophagy accelerates positive-strand RNA virus infection by increasing viral RNA translation, RNA replication, and virus particle production (50–54). Both DNA and RNA viruses were reported to regulate the autophagy pathway by modulation of their replication (54–59). Foot-and-mouth disease virus-triggered autophagy promotes viral replication through regulation of the EIF2S1-ATF4-AKT-mTOR pathway (58). *Avibirnavirus* infectious bursal disease virus-induced autophagy suppresses viral replication via the HSP90AA1–AKT-mTOR pathway (60). Previous studies have demonstrated that IAV infection induces autophagy depending on the AKT-TSC2-mTOR signaling pathway (61), and several viral proteins such as M2, hemagglutinin (HA), and NS1 are involved in initiating the

formation of autophagosomes in infected cells (62, 63). However, the role that autophagy plays during IAV replication is controversial and is cell type and virus strain dependent. In addition, whether other IAV proteins are able to induce autophagy and what the role of the IAV protein-host autophagy interaction in regulating IAV replication is remain unclear.

In this study, we investigated whether autophagy machinery is required for IAV replication and how it functions. We first showed that alteration of the autophagic level by pharmacological inhibitors/inducers or autophagy gene knockdown affects viral progeny production. Our studies further revealed that autophagy promotes influenza viral RNA translation and synthesis. Notably, our studies demonstrated that both IAV NP and M2 proteins induce autophagy by inhibiting the AKT-mTOR signaling pathway and by increasing HSP90AA1 expression. Finally, we noted that NP- and M2-induced autophagy functions in different stages of IAV replication to promote IAV replication through increasing the interaction of PB2 and HSP90AA1, vRNP export, and infectious viral particle formation in host cells.

RESULTS

Inhibition of autophagy decreases influenza virus replication. We first showed that the A/duck/Hubei/Hangmei01/2006(H5N1) (HM/06) virus was able to induce autophagosome accumulation at as early as 9 h postinfection (hpi) once the viral NP protein could be detected in virus-infected A549 cells, and the autophagosome accumulation increased gradually to 36 hpi with the NP protein accumulation, as evidenced by the results of Western blotting (Fig. 1A), which is in agreement with findings reported previously (62). These results also suggested that protein accumulation during IAV replication is essential for autophagy induction. Simultaneously, cell viability was evaluated by CCK-8 assay at the indicated time points and showed that HM/06 infection did not affect cell viability until 36 hpi (Fig. 1B). To determine the effect of autophagy on the replication of HM/06, we used multiple approaches to examine whether the autophagy machinery is essential for HM/06 replication; specifically, we used the infection of cells in which induction of autophagy was disrupted with a pharmacological inhibitor and infection of cells genetically deficient in the autophagy genes required for autophagy membrane formation. Treatment of cells with LY294002 (a PI3K inhibitor) before infection resulted in a significant reduction in viral yield compared to yield in nontreated cells at 12, 24, and 36 hpi (Fig. 1C). Similar results were obtained in cells treated with 3-methyladenine (3-MA), an inhibitor of autophagy (64) (Fig. 1D). Moreover, the autophagy gene ATG5, which is required for activating autophagy and is involved in one of the two ubiquitin-like conjugation systems mediating vesicle elongation during the autophagosome formation process (34), was knocked down before virus infection. As shown in Fig. 1E, ATG5 expression was efficiently knocked down, and the viral progeny titers were also dramatically decreased in the ATG5-knockdown cells compared with the levels at 12, 24, and 36 hpi in negative-control (NC) cells knocked down by a nontargeting small interfering RNA (siRNA). Similar results were also obtained in cells with knockdown of the common ubiquitin E1-like activating enzyme ATG7 (Fig. 1F), which is essential for the assembly and function of those two conjugates (ATG12-ATG5-ATG16 and LC3/ATG8) in the expansion of autophagosomal membranes.

To evaluate whether autophagy influenced protein expression, the autophagy was disrupted by applying LY294002 and knocking down ATG5 and BECN1/Beclin1 (which not only participates in autophagosome formation but also interacts with different protein complexes regulating the autophagosome-lysosome fusion [33]). Results showed that the expression levels of LC3-II as well as those of influenza viral proteins PB1, PB2, PA, NP, and M2 were reduced in LY294002-, ATG5-, and BECN1-treated HM/06-infected cells in comparison with levels in the nontreated cells (Fig. 2A to C). Simultaneously, LY294002 treatment and ATG5 knockdown in HM/06-infected cells significantly downregulated the viral NP mRNA, vRNA, and cRNA levels (Fig. 2D and E).

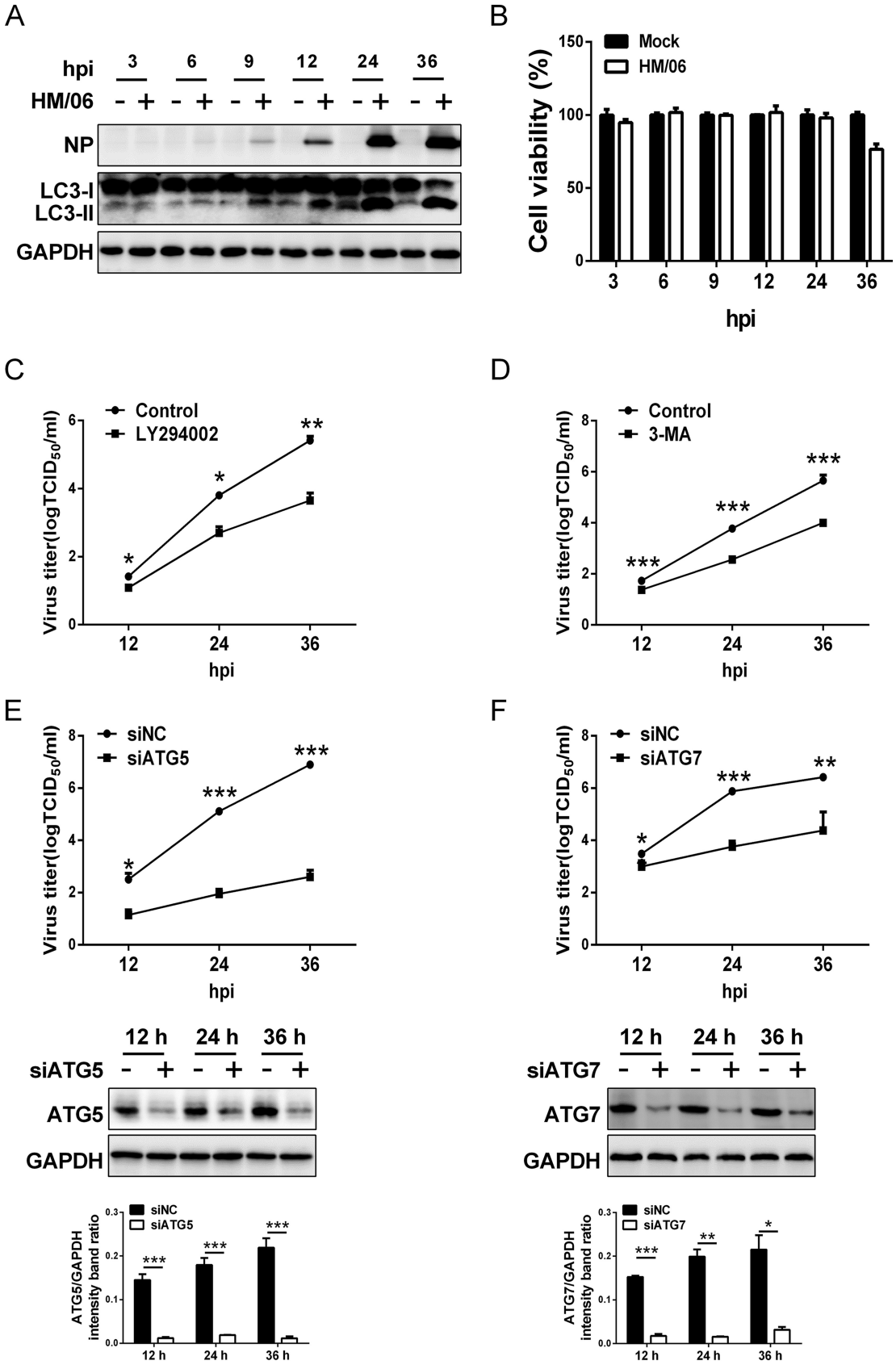

FIG 1 Inhibition of autophagy suppresses influenza HM/06 replication. (A) A549 cells were infected with the HM/06 virus at an MOI of 0.1. Cell lysates were collected at 3, 6, 9, 12, 24, and 36 hpi and were subjected to Western blot analysis. (B) A549 cells plated

(Continued on next page)

These results suggest that the cellular autophagy mechanism may support influenza virus replication.

Induction of autophagy with starvation or rapamycin increases influenza virus replication. To substantiate the role of autophagy in influenza virus replication, we analyzed viral NP expression and the viral progeny yields after rapamycin (an autophagy inducer) and starvation treatment, respectively. Results showed that both rapamycin and starvation treatments not only upregulated the expression of LC3-II and NP at 24 hpi in the HM/06 virus-infected A549 cells compared with the levels in nontreated cells (Fig. 3A) but also increased the yields of influenza viral progeny (Fig. 3B). These results suggest that the induction of autophagy before IAV infection promotes influenza virus replication.

Induction of autophagy with starvation and rapamycin promotes the viral life cycle or gene expression. To address which step(s) of the virus life cycle is regulated by autophagy, we performed a comprehensive and systematic dissection of the viral life cycle. First, we examined whether induction of autophagy was able to impair the early stages of the influenza virus life cycle. The effect of autophagy on viral entry, binding, and internalization was determined. The control or starvation- and rapamycin-pretreated A549 cells were incubated with the HM/06 virus at 37°C for 30 min and washed extensively to remove the uninternalized virions. M1, which has commonly been used as a marker of IAV internalization (65), was detected in the internalized virions by Western blotting. No significant difference was observed in the M1 and NP expression levels in either the starvation- or rapamycin-treated cells infected with the HM/06 virus compared with levels in the control-treated cells infected with the HM/06 virus (Fig. 4A). Simultaneously, the cell supernatants were also collected and analyzed by 50% tissue culture infective dose ($TCID_{50}$) assays to quantify the virus that did not enter the cells. Results showed that the virus titers were comparable in the starvation-, rapamycin-, and control-treated cells (Fig. 4B). These results suggest that autophagy has no effect on viral entry, binding, and internalization.

To further investigate a potential effect of modulation of autophagy on viral gene expression, NP expression was examined by Western blotting at 4 hpi. Results showed that the expression level of NP experienced a significant increase in both the starvation- and rapamycin-treated cells infected with the HM/06 virus in comparison with the level in the control-treated HM/06-infected cells (Fig. 4C). In addition, we also evaluated the effect of autophagy induction on influenza vRNA and cRNA replication and mRNA transcription by quantitative reverse transcription-PCR (qRT-PCR) at 4 hpi; results showed that starvation and rapamycin treatments resulted in slight but statistically significant upregulation in the copy numbers of M gene vRNA, cRNA, and mRNA compared with levels in cells with control treatment and infected with the HM/06 virus (Fig. 4D). Taken together, these results suggest that the enhancing effect of autophagy induction on viral replication occurs during the early stages of the viral life cycle or during viral RNA synthesis and protein expression.

Inhibition of autophagy impairs the early stages of the viral life cycle or viral RNA synthesis. To further verify the effect of the HM/06-induced autophagy on the early stages of virus infection, we disrupted autophagy by silencing ATG5 and BECN1. Results showed that the expression levels of LC3-II and viral proteins including PB1, PB2, PA, NP, and M2 were markedly downregulated in HM/06-infected ATG5- and BECN1-knockdown cells at 4 hpi in contrast to levels in the NC-knockdown cells (Fig. 5A and

FIG 1 Legend (Continued)
on the 96-well plates were prepared as described for panel A, and cell viability was detected by CCK-8 assay at the indicated time points postinfection. (C and D) A549 cells were pretreated with a control (DMSO) or 10 μM LY294002 (C) or 5 mM 3-MA (D) for 6 h and then infected with the HM/06 virus at an MOI of 0.1. Cell culture supernatants were collected at 12, 24, and 36 hpi. Virus titers were determined by $TCID_{50}$ assay on MDCK cells. (E and F) A549 cells were transfected with siATG5 or siATG7 for 36 h and then mock infected or infected with HM/06 at an MOI of 0.1. Cell culture supernatants were collected at 12, 24, and 36 hpi. Virus titers were determined as described for panels C and D. Expression of ATG5 or ATG7 protein was analyzed by Western blotting. siNC, nontargeting siRNA, negative control. Means and SD (error bars) of three independent experiments are indicated (*, $P < 0.05$; **, $P < 0.01$; ***, $P < 0.001$).

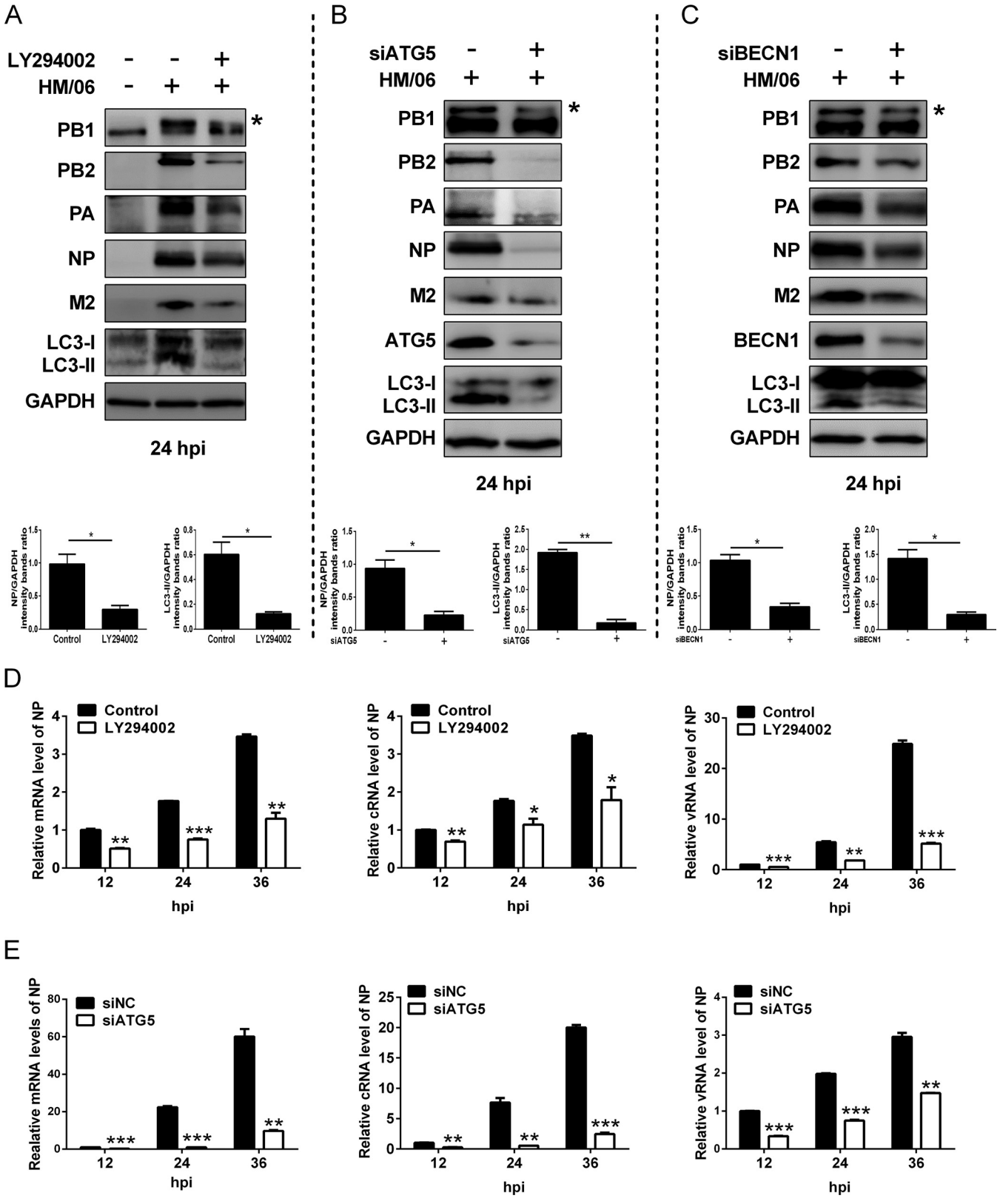

FIG 2 Inhibition of autophagy suppresses the influenza virus protein expression. (A to C) A549 cells treated with the LY294002, siATG5, or siBECN1 were mock infected or infected with the HM/06 virus. Cell lysates were harvested and analyzed by Western blotting (an asterisk next to the blot indicates the protein). (D and E) A549 cells were pretreated with LY294002 or siATG5 and mock infected or infected with the HM/06 virus. Cell lysates were collected at 12, 24, and 36 hpi. Then, total RNA was extracted, and the levels of NP gene vRNA, cRNA, and mRNA were measured by quantitative RT-PCR. GAPDH was used as a control for the normalization of cellular mRNA and intracellular viral RNA. Means and SD (error bars) were determined for triplicates of three independent experiments, and values were standardized to the levels of control-treated or siNC-infected cells at 12 hpi (*, $P < 0.05$; **, $P < 0.01$; ***, $P < 0.001$).

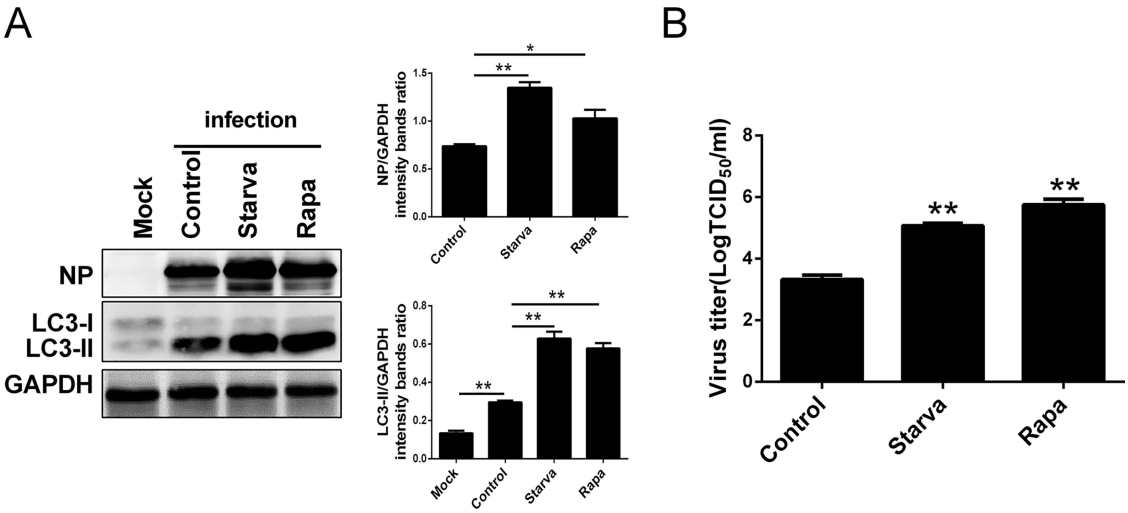

FIG 3 Induction of autophagy with starvation or rapamycin facilitates viral replication. (A) The culture medium of A549 cells was exchanged with Ham's F-12 medium without FBS for 6 h or pretreated with a control (DMSO) or 500 nM rapamycin for 12 h and then were mock infected or infected with HM/06 at an MOI of 0.1. At 24 hpi, cell lysates were collected and subjected to the Western blot analysis. (B) A549 cells were treated as described for panel A. Cell culture supernatants were collected, and virus titers were determined by $TCID_{50}$ assay. Means and SD (error bars) of three independent experiments are indicated (*, $P < 0.05$; **, $P < 0.01$).

B). Similar results were obtained in the LY294002-treated cells (Fig. 5C). These results suggest that suppressing autophagy depressed viral protein expression in the early stages of the viral life cycle. Further studies showed that significant reductions in the M gene vRNA and mRNA levels were detected in A549 cells treated with an siRNA targeting ATG5 (siATG5) and LY294002 and infected with the HM/06 virus at 4 hpi (Fig. 5D), indicating that autophagy truly upregulates viral RNA synthesis. Moreover, the effect of autophagy on viral polymerase activity was further investigated by using an influenza virus minireplicon system. As shown in Fig. 5E, knocking down ATG5 remarkably suppressed luciferase reporter enzymatic activity (~1.51-fold), suggesting that autophagy increases the viral polymerase activity. To examine whether autophagy could influence vRNP export to the cytoplasm, NP subcellular localization was analyzed during the indicated time course of infection of siATG5-treated A549 cells (Fig. 5F). At 4 hpi, as expected for an intermediate time point in the virus life cycle, NP was observed to be located mainly in the nucleus in both siNC- and siATG5-treated cells. For both siNC- and siATG5-treated cells, though the amount of nuclear NP decreased with time as NP was progressively exported to the cytoplasm, export of NP from nucleus to the cytoplasm was delayed in the ATG5-knockdown cells in contrast to the level in NC-knockdown cells; this might reflect the reduction of newly synthesized viral NP protein in the nucleus of the infected cells, suggesting that autophagy promotes vRNP export to the cytoplasm. Taken together, these results indicate that the enhancing effect of autophagy on viral replication occurs during viral RNA synthesis.

IAV NP and M2 proteins induce autophagy and interact with LC3. Because we have shown that autophagy promotes influenza viral gene expression and RNA synthesis, we speculated that the IAV-host autophagy interaction plays a critical role in regulating IAV replication. NP is associated with viral RNA and RdRp and acts as a key structural determinant of vRNP (5, 6), and M2 is able to induce autophagosome accumulation (62). Thus, the localization of influenza viral M2 and NP proteins with GFP-LC3 puncta was analyzed by immunofluorescence analysis in HM/06 virus-infected cells. Results showed that the GFP-LC3 fluorescence was evenly distributed in the nucleus and cytoplasm in mock-infected cells (Fig. 6A, top row), whereas HM/06 virus infection resulted in LC3 transportation from the nucleus to the cytoplasm and induced formation of large LC3 puncta in the cytoplasm (Fig. 6A), indicating the HM/06 virus infection induces autophagosome accumulation, as reported above (Fig. 1A). Of note, the influenza viral M2 protein colocalized very well with the LC3 puncta mainly in the

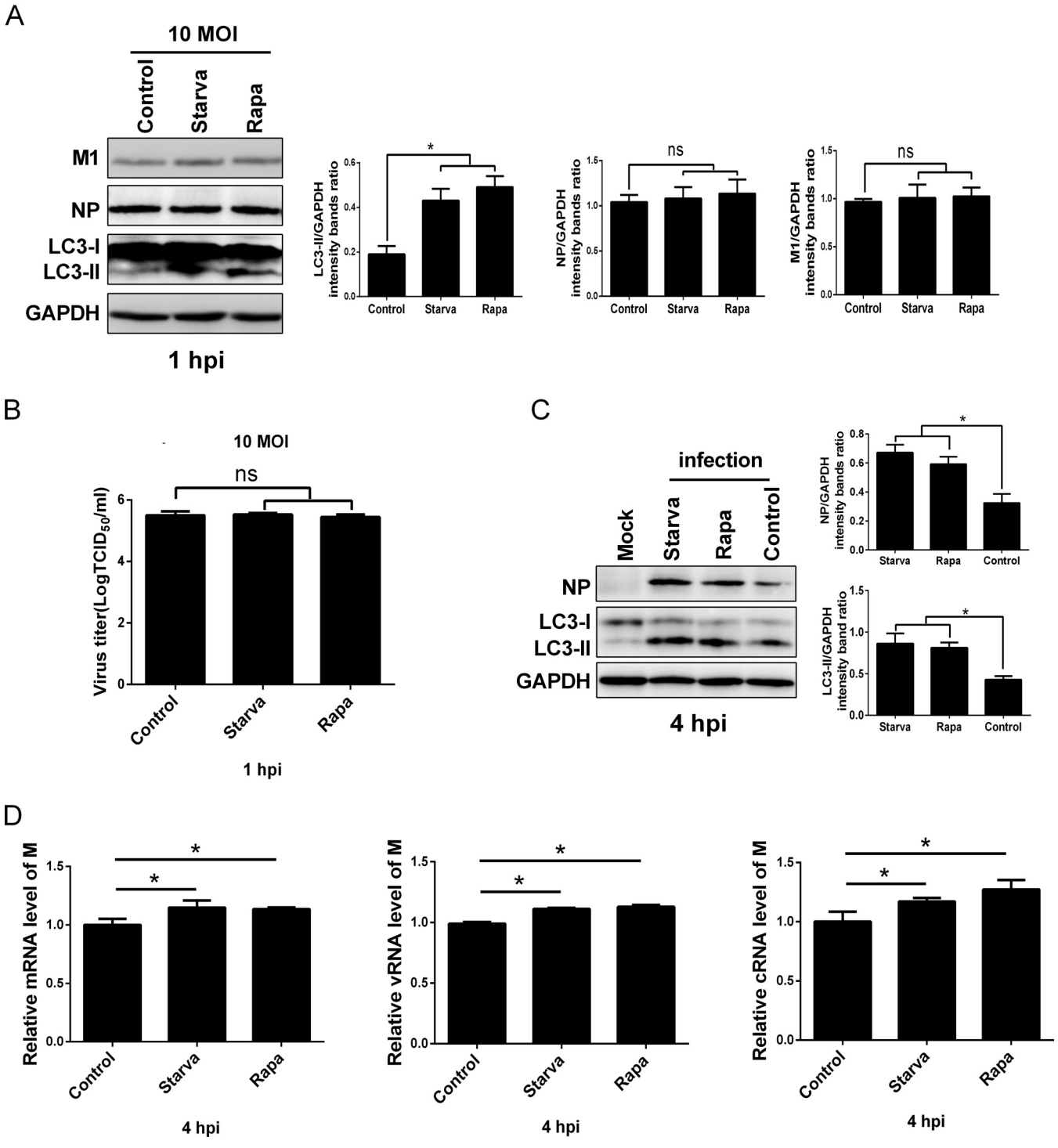

FIG 4 Induction of autophagy promotes the early stages of the viral life cycle or viral gene expression. (A and B) The culture medium of A549 cells was exchanged with Ham's F-12 medium without FBS for 6 h or pretreated with rapamycin for 12 h and then incubated with the HM/06 virus at an MOI of 10 for 30 min (at 37°C). Cells were washed with PBS-HCl (pH 1.3) to remove all attached virions from the surface of A549 cells. Cell lysates were collected for Western blot analysis (A), and cell culture supernatants (noninfectious virus particles) were collected and determined by $TCID_{50}$ assay (B). (C) A549 cells were treated as described for panels A and B and then were mock infected or infected with the HM/06 virus for 4 h. Lysates were harvested and analyzed by Western blotting. (D) A549 cells were treated as described for panels A and B and infected with the HM/06 virus for 4 h. The levels of M mRNA, vRNA, and cRNA were determined by RT-PCR. GAPDH was used as a control for the normalization of cellular mRNA and intracellular viral RNA. Means and SD (error bars) were determined for triplicates of three independent experiments and were standardized to the levels of control-infected cells at 4 hpi (*, $P < 0.05$; ns, nonsignificant).

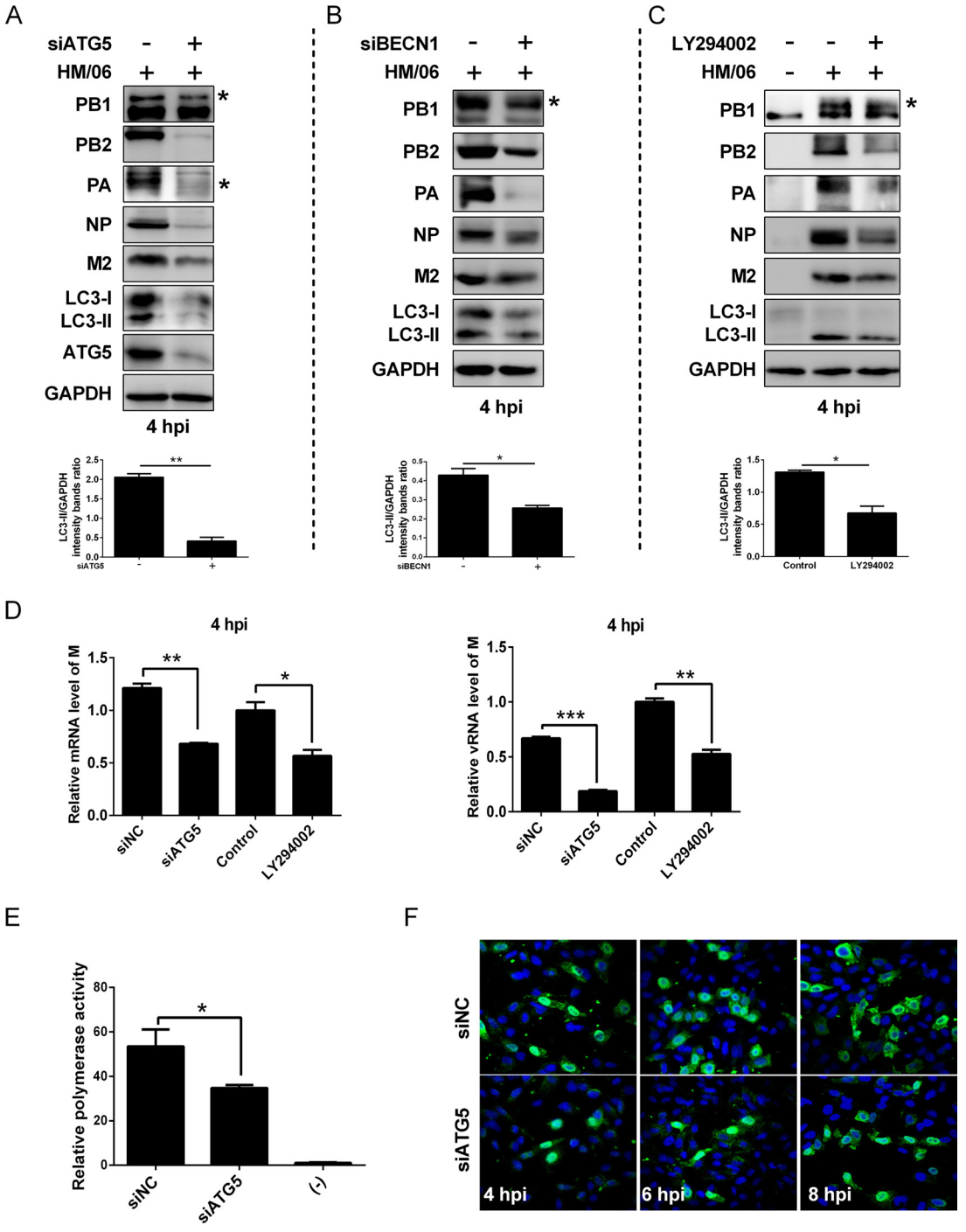

FIG 5 Inhibition of autophagy disrupts the early stages of the viral life cycle or viral RNA synthesis. (A and B) A549 cells were transfected with siATG5 or siBECN1, as indicated, for 36 h and then were infected with the HM/06 virus. After 4 hpi, cell lysates were collected for Western blot analysis. An asterisk next to the blot indicates the protein. (C) A549 cells were pretreated with LY294002 for 6 h and then were mock-infected or infected with the HM/06 virus for 4 h. Cells were harvested and analyzed by Western blot. An asterisk next to the blot indicates the protein. (D) siATG5- or LY294002-pretreated A549 cells were mock infected or infected with the HM/06 virus for 4 hpi. M mRNA and vRNA levels were determined by RT-PCR. GAPDH was used as a control for the normalization of cellular mRNA and intracellular viral RNA. Means and SD were determined for triplicates of three independent experiments and were standardized to the levels of control-infected cells at 4 hpi. (E) HEK 293T cells were transfected with siATG5. Twelve hours later, cells were further transfected with plasmids encoding the polymerase complex components and NP derived from influenza HM/06 virus, along with a reporter plasmid containing the noncoding sequence from the NP segment as well as the luciferase gene driven by the human polymerase I promoter. Luciferase activity was determined at 36 h posttransfection, and relative activities were compared. (F) A549 cells treated with the indicated siRNAs were infected with the HM/06 virus at an MOI of 10. Cells were fixed at 4, 6, and 8 hpi for immunostaining of NP as a marker for vRNP complex export, and nuclei were stained using 4′,6′-diamidino-2-phenylindole, and then visualized by confocal microscopy. Means and SD (error bars) of three independent experiments are shown (*, $P < 0.05$; **, $P < 0.01$; ***, $P < 0.001$).

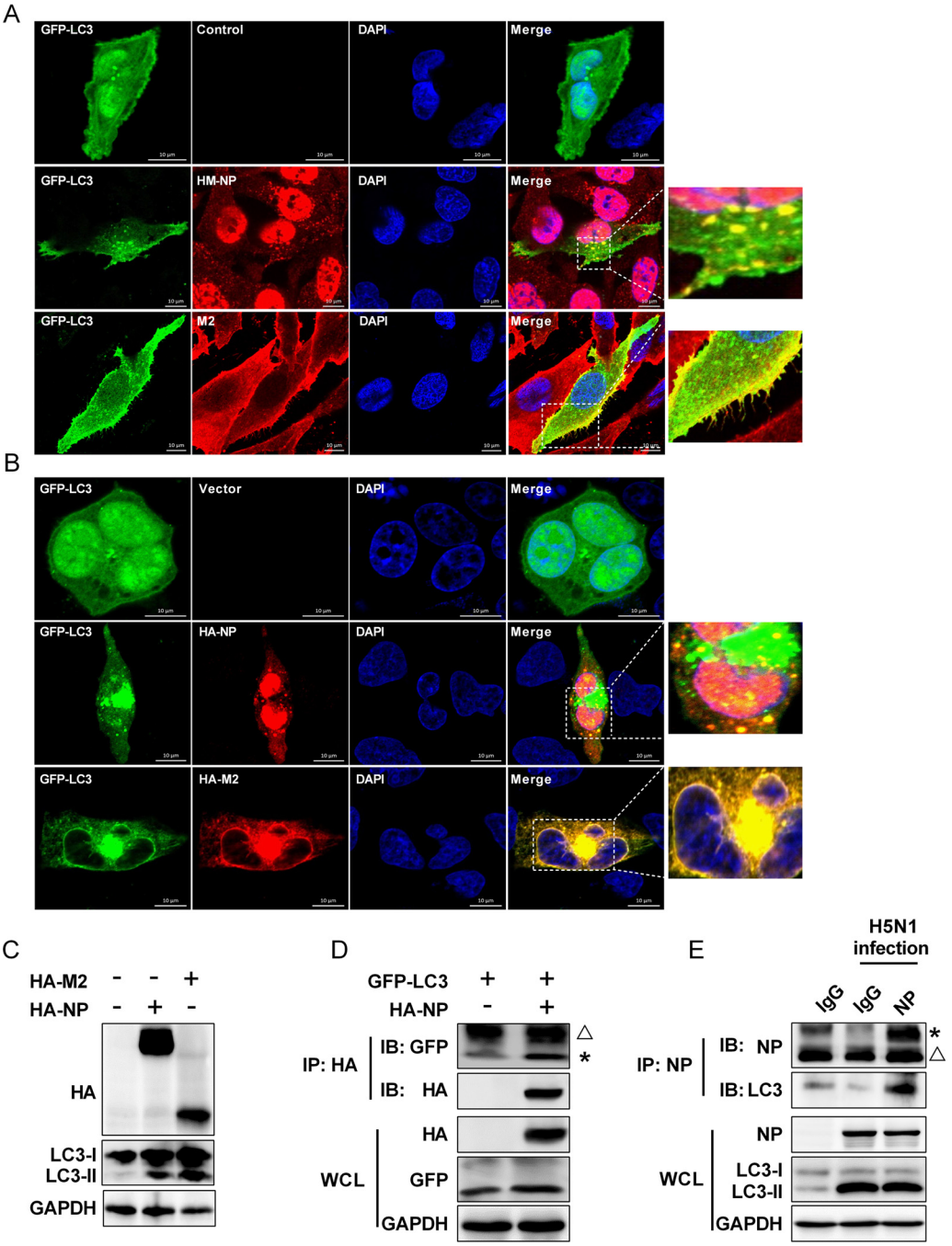

FIG 6 IAV NP and M2 proteins induce autophagy and interact with LC3. (A) A549 cells were transfected with GFP-LC3 for 24 h and then were mock-infected or infected with the HM/06 virus. Twenty-four hours later, cells were fixed and stained with anti-NP or -M2 antibody and then visualized by confocal microscopy. In the zoomed images, yellow spots indicate the merging of M2 or NP with LC3 puncta. The image is representative of 20 cells. Scale bar, 10 μm. (B) A549 cells were cotransfected with GFP-LC3 and HA-M2 or HA-NP. After 24 h, cells were fixed and stained with anti-HA antibody and then visualized by confocal microscopy. In the zoomed images, yellow spots indicate the merging of M2 or NP with LC3 puncta. The image is representative of 20 cells. Scale bar, 10 μm. (C) HEK 293T cells were transfected with the indicated plasmids for 24 h, and cells lysates were collected for Western blot analysis. (D) HEK 293T cells were transfected with the indicated plasmids for 24 h. Cell lysates were immunoprecipitated with anti-HA antibody and then analyzed by Western blotting. (E) Lysates of HM/06-infected A549 cells were prepared, immunoprecipitated with the anti-NP antibody or control IgG, and then subjected to Western blot analysis. An asterisk next to the blot indicates the protein, the triangle indicates the heavy chain. Results are representative of three independent experiments. WCL, whole-cell lysate; IP, immunoprecipitation; IB, immunoblotting; DAPI, 4′,6′-diamidino-2-phenylindole.

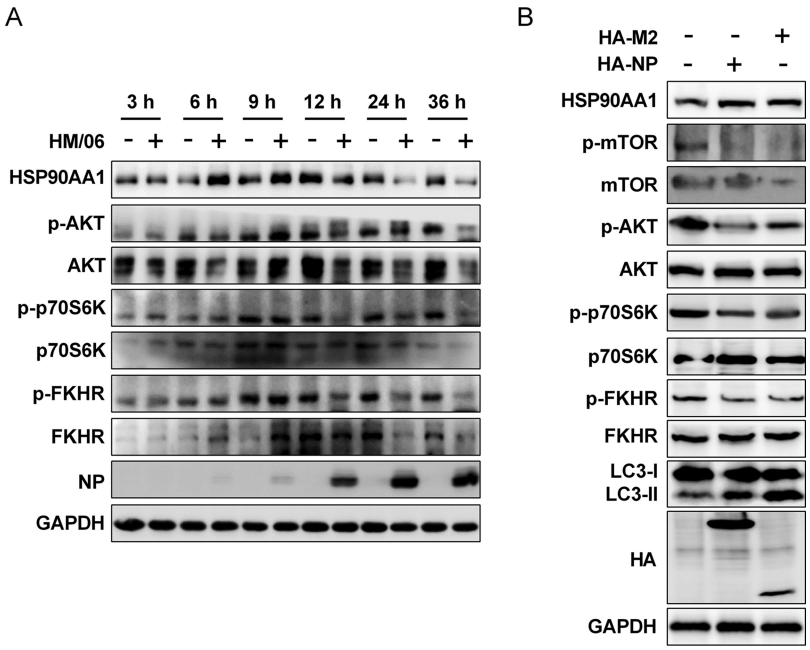

FIG 7 IAV NP and M2 induce autophagy via the AKT-mTOR pathway. (A) A549 cells were prepared as described in the legend of Fig. 1A, and the cell lysates were analyzed by Western blotting. (B) HEK 293T cells were transfected with HA-NP or HA-M2 for 24 h, and cell lysates were collected and subjected to Western blot analysis. Results are representative of three independent experiments.

plasma membrane (Fig. 6A, bottom row), whereas the NP protein colocalized with the LC3 puncta mainly in the perinuclear region (Fig. 6A, middle row), indicating that influenza viral M2 and NP may regulate the autophagic process to promote IAV replication at different stages of IAV replication. To substantiate this, immunofluorescence analysis was performed to determine whether NP and M2 expression could induce autophagosome formation. As shown in Fig. 6B, M2 expression induced formation of multiple LC3 puncta, and M2 colocalized very well with the LC3 puncta, which was consistent with previously reported findings (62). Intriguingly, the results also showed that cells transfected with NP resulted in LC3 punctum accumulation, and NP partially colocalized with the LC3 puncta in the cytoplasm. Moreover, the conversion of LC3-I to LC3-II was further analyzed in NP-transfected cells (with M2 as a positive control) by Western blotting. As shown in Fig. 6C, the level of endogenous LC3-II was significantly increased in the NP- and M2-transfected cells in comparison with the level in the control-transfected cells. These results suggest that NP overexpression is able to induce autophagy. The interaction of LC3 and M2 is required for IAV budding and virus stability (62). NP is an important component of the influenza vRNP complex; since our studies have established that autophagy promoted the nuclear export of influenza vRNP, we hypothesized that NP also physically interacted with LC3. As expected, results of coimmunoprecipitation (co-IP) assays showed that HA-NP physically interacted with GFP-LC3 (Fig. 6D). Importantly, NP also coimmunoprecipitated with endogenous LC3 in HM/06-infected A549 cells (Fig. 6E). These results suggest that the colocalization and interaction of LC3 with NP are possibly beneficial for the nuclear export of the vRNP, thereby leading to an increase in influenza virus replication.

IAV NP and M2 proteins induce autophagy via the AKT-mTOR pathway. IAV induces autophagy via an AKT-mTOR signaling pathway (61), which is reported to be crucial for protein synthesis (66). Here, we also determined whether the HM/06 virus induces autophagy by regulating the AKT-mTOR pathway. As shown as in Fig. 7A, HM/06 virus infection resulted in time course changes in the levels of AKT and phosphorylation of both its downstream substrate FKHR (Ser256) and p70S6K (Thr389) (a downstream effector of mTOR signaling) in A549 cells. The levels of total AKT, FKHR,

and p70S6K and phosphorylated AKT, FKHR, and p70S6K were time-dependently decreased from 12 to 36 hpi, indicating that autophagy was induced by HM/06 virus infection through the AKT-mTOR pathway. In contrast, the levels of phosphorylated AKT, FKHR, and p70S6K increased from 6 hpi and peaked at 9 hpi, demonstrating that an increase in AKT-mTOR signal occurred as an early response to IAV infection to support the viral protein accumulation.

Because NP and M2 were able to induce autophagy (Fig. 6C), we next determined whether NP and M2 mediated autophagy efficiently through the AKT-mTOR pathway. Results showed that the phosphorylation levels of AKT, mTOR, FKHR, and pS706K were significantly downregulated in either NP- or M2-transfected cells although the levels of whole AKT, mTOR, FKHR, and p70S6K were comparable in NP, M2, and control-transfected HEK 293T cells (Fig. 7B). Taken together, these results suggest that NP- and M2-induced autophagy is dependent on the AKT-mTOR pathway.

Autophagy promotes IAV RNA synthesis by regulating HSP90AA1 expression. Influenza virus RNA synthesis occurs in the nucleus of infected cells, and the efficient transcription/replication of the viral genome is dependent on host factors. A couple of cellular proteins, including HSP90AA1, have been identified as host factors involved in influenza viral RNA synthesis, including nuclear import and assembly of vRNPs (67, 68). Moreover, HSP90AA1 maintains PI3K/AKT activity by interacting with AKT (69). We have shown that the accumulation of vRNA and viral proteins was suppressed by the PI3K inhibitors, suggesting that the PI3K/AKT pathway may modulate influenza vRNA synthesis, and the host factor HSP90AA1 could be a potential target for the PI3K/AKT signaling to facilitate the vRNA synthesis. As expected, HSP90AA1 exhibited an increase at 6 hpi and 9 hpi but a reduction from 12 hpi to 36 hpi in HM/06-infected cells (Fig. 7A), indicating that HSP90AA1 accumulated at the early stages of viral infection to support influenza viral RNA synthesis. Intriguingly, we showed that NP and M2 overexpression led to an obvious upregulation in the HSP90AA1 level (Fig. 7B). Furthermore, the induction of HSP90AA1 expression by NP was markedly suppressed in the ATG5-knockdown cells compared with the level in the NC-knockdown cells (Fig. 8A). These results demonstrated that autophagy induction increases HSP90AA1 expression in response to NP overexpression. To validate whether NP-induced autophagy is associated with HSP90AA1, we examined the autophagy level following NP transfection with the siRNA targeting HSP90AA1. Results showed that the NP-induced LC3-II increase was significantly depressed in HSP90AA1-knockdown cells compared to that of the NC-knockdown cells (Fig. 8B), suggesting that NP-induced autophagy is regulated by HSP90AA1.

The IAV polymerase complex consisting of three subunits (PA, PB1, and PB2) is essential for viral RNA replication and transcription (8), and HSP90AA1 was reported to interact with PB2 to promote influenza vRNP complex formation and vRNA synthesis within the nucleus (67, 68, 70). Next, we determined in our study whether PB2 interacts with the host HSP90AA1. Results of co-IP assays showed that PB2 coimmunoprecipitated with the endogenous HSP90AA1 (Fig. 8C). Taken together, these results suggest that NP and M2 mediate autophagy induction by modulating HSP90AA1 expression, resulting in an increase of the binding of HSP90AA1 to PB2, which promotes IAV RNA synthesis and thereby favors viral replication.

DISCUSSION

Autophagy is reported to be involved in influenza A virus replication (45), but the underlying mechanisms have thus far remained unclear. Here, we demonstrate that induction of autophagy with starvation and rapamycin treatment and suppression of autophagy by applying pharmacological inhibitors or siRNA affect influenza viral replication. Our studies further show that autophagy accelerates the viral polymerase activity, resulting in an increase in viral RNA synthesis and nuclear export of vRNP; this, in turn, leads to an increase in the accumulation of the viral proteins and to the upregulation of viral progeny production. Previous reports showed that treatment with

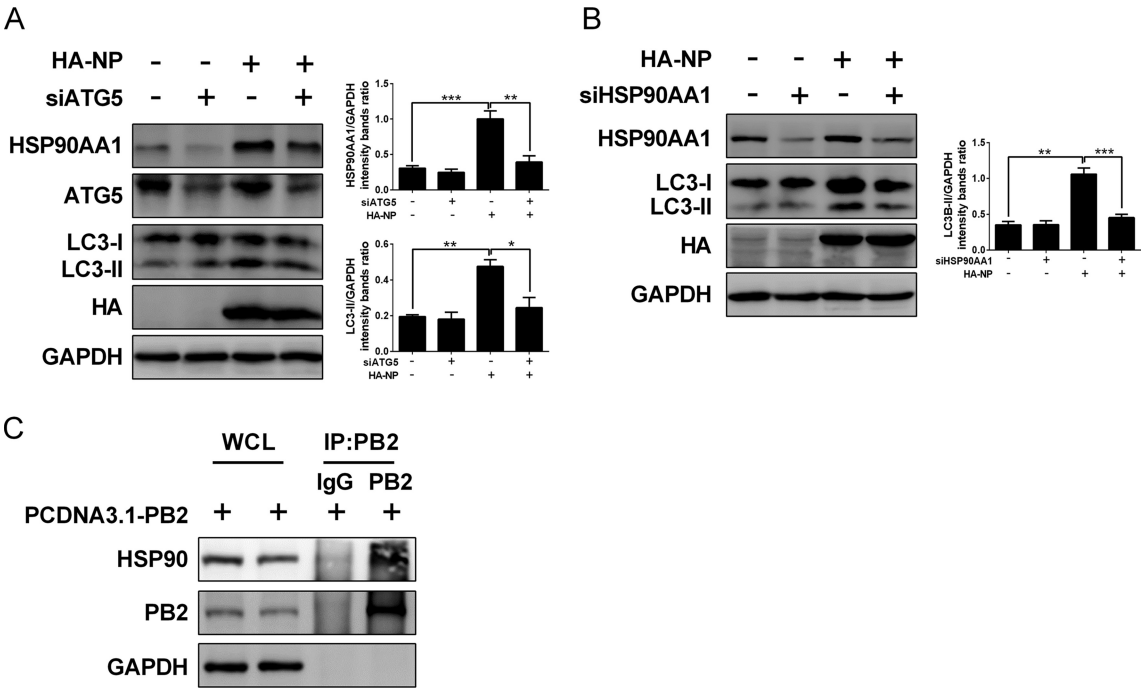

FIG 8 Autophagy facilitates IAV RNA synthesis by regulating HSP90AA1 expression. (A) HEK 293T cells were transfected with siATG5 for 36 h and then transfected with the indicated plasmids. Twenty-four hours later, cell lysates were harvested for Western blot analysis. (B) siHSP90AA1-transfected HEK 293T cells were transfected with indicated plasmids for 24 h, and lysates were subjected to Western blot analysis. (C) Lysates of PCDNA3.1-PB2-transfected HEK 293T cells were prepared and immunoprecipitated with the anti-PB2 antibody or control IgG, and then cells were subjected to Western blot analysis. Results are representative of three independent experiments.

PI3K inhibitors does not impair the synthesis of viral RNAs (45, 71, 72); the present results might be due to a difference in the virus strain and cell type used in our study.

During viral infection, the virus-host autophagy interaction plays a critical role in the host response to infection and viral pathogenicity (60). It has been proposed that autophagic intracellular membranes can serve as a structural platform for viral genome replication and assembly (43, 49, 73, 74). NP, an important subunit of vRNP complex, is involved in IAV assembly (5, 6). Here, we demonstrate that the IAV NP protein, when expressed alone or during virus infection, colocalizes well with the autophagy marker protein LC3 in the cytoplasm and mainly in the perinuclear region. Moreover, NP can physically interact with LC3 in both virus-infected cells and in cells coexpressing LC3; suppressing IAV infection-induced autophagy decreases vRNP export, which suggests that autophagy accelerates vRNP export by colocalizing with LC3 at the perinuclear region and interacting with LC3, thereby promoting IAV replication. In agreement with a previous study which showed that the interaction of M2 with LC3 is required for virus budding and stable viral progeny (62), our study also demonstrated that IAV M2 protein colocalizes well with LC3, which further supports the beneficial role of autophagy in IAV replication. The IAV polymerase complex consisting of three subunits (PA, PB1, and PB2) is essential for viral RNA replication and transcription (8), and HSP90AA1 has been identified as a host factor to interact with PB2 to promote influenza vRNA synthesis, including nuclear import and assembly of vRNPs (67, 68, 75). Similarly, the interaction of PB2 and HSP90AA1 also was identified in our study. Furthermore, HSP90AA1 maintains PI3K/AKT activity by binding to AKT (69), and the AKT-mTOR pathway is crucial for protein synthesis and the regulation of autophagy (66). In this study, we show that NP and M2 upregulated HSP90AA1 expression, which modulated NP- and M2-mediated autophagy through the AKT-mTOR signaling pathway. These results indicate that NP- and M2-mediated autophagy increases HSP90AA1 expression, leading to more binding of PB2 to HSP90AA1, which results in an increase in vRNA synthesis. It has been documented that IAV M2 blocks the autophagosome fusion with lysosome

(62), and IAV infection induced autophagy as early as 9 hpi once NP protein could be detected in our study. Thus, it is most likely that IAV NP and M2 mediate autophagosome accumulation by upregulating HSP90AA1 expression and regulating the AKT-mTOR signaling pathway at early time points of infection, which favors viral RNA synthesis via the increase of the interaction of PB2 and HSP90AA1 and promotes vRNP export through subsequent binding of NP to LC3; later in the replication cycle this interferes with lysosomal targeting of autophagic vesicles to favor the production of infectious viral particles through the interaction of M2 and LC3. However, the expression level of HSP90AA1 decreased at late stages of viral infection, possibly due to the host responses to counteract extensive virus production leading to pathogenicity.

In conclusion, our study unveils a novel mechanism utilized by IAV to promote its replication and provides new insight into pathogenicity of IAV. We conclude that NP and M2 mediate autophagy through regulation of HSP90AA1 expression and the AKT-mTOR signaling pathway, which functions in different stages of viral replication to promote the IAV replication. Moreover, improved understanding of IAV replication in the host cell may facilitate development of novel antiviral therapeutics for the prevention and control of influenza virus infection.

MATERIALS AND METHODS

Cells and virus. The human lung epithelial cell line A549 and Madin-Darby canine kidney (MDCK) cells were obtained from the China Center for Type Culture Collection (Wuhan, China), and human embryonic kidney (HEK) 293T cells were purchased from ATCC (Manassas, VA, USA). Cells were maintained in Ham's F-12 medium, Dulbecco's modified Eagle's medium (DMEM; HyClone, China), and RPMI 1640 medium (HyClone, China), respectively. They were supplemented with 10% heat-inactivated fetal bovine serum (FBS) (PAN Biotech, Germany) and incubated in a 37°C humidified incubator with 5% CO_2. A/duck/Hubei/Hangmei01/2006(H5N1) (HM/06) was isolated from duck brain tissues and stored in our laboratory. Viral titers were determined by 50% tissue culture infectious dose ($TCID_{50}$) analysis on MDCK cells. Briefly, A549 cells were infected with HM/06 at a multiplicity of infection (MOI) of 0.1 or 10. After 1 h of adsorption, cells were washed once with warm phosphate-buffered saline (PBS) and then incubated in Ham's F-12 medium containing 1% FBS at 37°C. Virus stocks were collected at 1, 12, 24, and 36 hpi and serially diluted in DMEM and adsorbed onto confluent MDCK cells for 1 h at 37°C. Later, the inoculum was removed, and cells were washed twice with PBS and cultured with DMEM containing 1% FBS. After 3 days of incubation, virus titers were determined by calculating $\log_{10}$ $TCID_{50}$/milliliter on MDCK cells using the method developed by Reed and Muench (76). All experiments with HM/06 were performed in a biosafety level 3 laboratory at Huazhong Agricultural University.

Antibodies and reagents. Rabbit polyclonal anti-BECN1/Beclin 1, HSP90AA1, and control IgG (A7353, A0365, and AC005; ABclonal Biotechnology, Cambridge, MA, USA), rabbit monoclonal anti-ATG7 (8558S; Cell Signaling Technology), mouse monoclonal anti-ATG5 (ARG54822; Arigo Biolaboratories, Taiwan), mouse monoclonal anti-glyceraldehyde-3-phosphate dehydrogenase (GAPDH) (CB100127; California Bioscience, Coachella, CA, USA), rabbit polyclonal anti-IAV PB1, PB2, PA, NP, M1, and M2 (GTX125923, GTX125926, GTX118991, GTX30852, GTX125928, and GTX125951; Gene Tex, USA), rabbit polyclonal anti-MAP1LC3B/LC3B (NB100-2220; Novus Biologicals, USA), mouse monoclonal anti-HA tag (M180-3; MBL), mouse monoclonal anti-Flag tag (F1804; Sigma-Aldrich, Saint Louis, MO, USA), and GFP (CW0258A; CWBio) antibodies were incubated overnight at 4°C. Horseradish peroxidase (HRP)-conjugated anti-rabbit and anti-mouse (BF03008 and BF03001; Beijing Biodragon Inmmunotechnologies, China) secondary antibodies were incubated for 1 h at room temperature. Alexa Fluor 488- or 594-conjugated goat anti-mouse (GM200G-02C and GM200G-43C; Sungene Biotech) or anti-rabbit (GR200G-02C and GM200G-43C; Sungene Biotech) secondary antibodies were incubated for 1 h at room temperature. Cells were incubated with dimethyl sulfoxide (DMSO) (D4540; Sigma-Aldrich), LY294002 (L9908; Sigma-Aldrich), 3-MA (M9281; Sigma-Aldrich), and rapamycin (553210; Sigma-Aldrich) at the corresponding concentrations (Fig. 1 and 3).

Plasmids and siRNA oligonucleotides. Full-length cDNAs encoding HM/06 NP, M2, and PB2 proteins were amplified by reverse transcription-PCR (RT-PCR) from total RNA extracted from A549 cells infected with HM/06 using specific primers (available upon request) and cloned into HA-pCAGGS (HA-NP and HA-M2) or PCDNA3.1 (PCDNA3.1-PB2). Plasmids encoding PB1, PB2, PA, and NP of HM/06 virus and plasmid GFP-LC3 were stored in our laboratory. The luciferase reporter plasmid pPolI-NP-Luc (pNP-Luc) was kindly provided by Hualan Chen (Harbin Veterinary Research Institute). RNA interference (RNAi) oligonucleotide 5′-GATTCATGGAATTGAGCCA-3′ was used for the ATG5, 5′-CAGUUUGGCACAAUCAAU A-3′ was used for the BECN1, 5′-GAAGAUAACAAUUGGUGUAUUdTdT-3′ was used for the ATG7, and 5′-CUACAAUUCCUCUGAUAAU-3′ was used for the HSP90AA1 siRNA experiments.

Coimmunoprecipitation and Western blotting. Whole-cell extracts were prepared in mammalian cell lysis buffer (CW0889; CWBio) or cell lysis buffer for Western blotting and immunoprecipitation (P0013; Beyotime) containing protease inhibitor cocktail (04693132001; Roche, Basel, Switzerland). The proteins detected (Fig. 1 to 8) were separated on SDS-PAGE gels and then electrotransferred onto nitrocellulose membranes (10600001 and 10600002; GE Healthcare Life Sciences), which were blocked for 1 h at room temperature in Tris-buffered saline with Tween (TBST) containing 2% bovine serum

albumin (BSA), and then the membranes were incubated with the indicated primary antibodies at 4°C overnight and then with the corresponding secondary antibodies conjugated to horseradish peroxidase at room temperature for 1 h. The signals were detected by using a WesternBright ECL detection kit (K-12045-D50; Advansta, USA) in an ECL detection system (Amersham Biosciences, Piscataway, NJ, USA).

Immunofluorescence analysis. A549 cells were transfected with the plasmids indicated in Fig. 6A and B and mock infected or infected with the HM/06 virus. At 24 h postinfection (or 24 h posttransfection), cells were washed with phosphate-buffered saline (PBS) and then fixed with 4% paraformaldehyde for 30 min at room temperature. Cells were then washed three times with PBS and incubated with 0.1% Triton X-100 for 10 min. Next, 2% BSA was used to block samples for 2 h, and then specific primary antibodies were incubated at 4°C overnight, followed by incubation with Alexa Fluor 488- and 594-conjugated goat anti-mouse or anti-rabbit secondary antibodies for 2 h. The cells were then observed by confocal microscopy (Carl Zeiss LSM 880 confocal microscope and ZEN lite, version 2.3, software).

Polymerase activity analysis. siRNA-treated HEK 293T cells were cotransfected with the luciferase reporter plasmid pPolI-NP-Luc (pNP-Luc) together with plasmids encoding PB1, PB2, PA, and NP of HM/06 virus. In addition, an internal control plasmid expressing *Renilla* luciferase (pGL4.75 hRluc/CMV) (Promega) was also cotransfected. Cells were lysed at 36 h posttransfection, and firefly luciferase and *Renilla* luciferase activities were determined with a dual-luciferase reporter assay system (E1910; Promega) according to the manufacturer's protocol. Means and standard deviations were determined for three independent experiments, and values were standardized to the activities of PB1-deleted polymerase.

Quantitative RT-PCR assay. siRNA-, LY294002-, starvation-, or rapamycin-treated A549 cells were mock infected or infected with the HM/06 virus at an MOI of 0.1 or 10. In Fig. 2, 4, and 5, total RNA was extracted using TRIzol (15596018; Invitrogen, Carlsbad, CA, USA) according to the manufacturer's instructions at the indicated hours postinfection, and 1 μg of RNA was reverse transcribed. For the detection of vRNA and cRNA, a vRNA- or cRNA-specific primer was used in the reverse transcription (RT) reaction mix, whereas for mRNA detection, an oligo(dT) primer was used. For quantification of NP and M vRNA, cRNA, and mRNA, a SYBR green-based real-time PCR method (Roche) was performed with an ABI ViiA 7 PCR system (Applied Biosystems, Foster City, CA, USA). Means and standard deviations were determined for three independent experiments, and expression of each gene was normalized to that of GAPDH. The primers used in this study are available upon request.

Cell viability assay. Cell viability assays were performed using a cell counting kit (CCK-8; Dojindo Molecular Technologies). A549 cells were plated in 96-well plates and cultured for 12 h. At a confluence of 100%, cells were then infected or mock infected with the HM/06 virus at an MOI of 0.1. Cell viability was analyzed at 3, 6, 9, 12, 24, and 36 hpi. In brief, cells were incubated at 37°C for 4 h by the addition of CCK-8 reagent according to the manufacturer's protocol. Relative viability was determined by calculating the optical density at 450 nm (OD_{450}) of infected cells normalized to that of mock-infected cells.

Starvation or rapamycin treatment. For the starvation treatment experiments, A549 cell culture medium was exchanged with Ham's F-12 medium without FBS for 6 h, and then cells were infected with the HM/06 virus. For rapamycin treatment experiments, A549 cells were pretreated with a control or 500 μM rapamycin and then infected with the HM/06 virus.

Statistical analyses. Data are expressed as means ± standard deviations (SD). Statistical analysis was performed by a paired two-tailed Student's *t* test. A *P* value equal to or lower than 0.05 was considered significant.

ACKNOWLEDGMENTS

We thank Xiao Xiao for critically proofreading the manuscript.

This study was supported by the National Key Research and Development Program (grants 2016YFD0500205 and 2016YFC1200201), Fundamental Research Funds for the Central Universities (2662017PY029), National Natural Science Foundation of China (grants 31761133005, 31572545, and 31772752), the Outstanding Youth Science Foundation of Hubei Province (2016CFA056).

H.Z., R.W., and Y.Z. designed the experiments, analyzed and organized data, and wrote the paper; R.W., Y.Z., J.Z., and C.R. performed the experiments; P.L., H.C., and M.J. helped construct mutants and contributed reagents/materials/analysis tools. All authors discussed the results and read the manuscript.

REFERENCES

1. Nguyen-Van-Tam JS. 2015. Influenza and other respiratory viruses. From the Editor's desk. Influenza Other Respir Viruses 9:99–100. https://doi.org/10.1111/irv.12311.
2. Molinari N-AM, Ortega-Sanchez IR, Messonnier ML, Thompson WW, Wortley PM, Weintraub E, Bridges CB. 2007. The annual impact of seasonal influenza in the US: measuring disease burden and costs. Vaccine 25:5086–5096. https://doi.org/10.1016/j.vaccine.2007.03.046.
3. Moeller A, Kirchdoerfer RN, Potter CS, Carragher B, Wilson IA. 2012. Organization of the influenza virus replication machinery. Science 338:1631–1634. https://doi.org/10.1126/science.1227270.
4. Murti KG, Webster RG, Jones IM. 1988. Localization of RNA polymerases on influenza viral ribonucleoproteins by immunogold labeling. Virology 164:562–566. https://doi.org/10.1016/0042-6822(88)90574-0.
5. Portela A, Digard P. 2002. The influenza virus nucleoprotein: a multifunctional RNA-binding protein pivotal to virus replication. J Gen Virol 83:723–734. https://doi.org/10.1099/0022-1317-83-4-723.

6. Noda T, Kawaoka Y. 2010. Structure of influenza virus ribonucleoprotein complexes and their packaging into virions. Rev Med Virol 20:380–391. https://doi.org/10.1002/rmv.666.
7. Te Velthuis AJW, Fodor E. 2016. Influenza virus RNA polymerase: insights into the mechanisms of viral RNA synthesis. Nat Rev Microbiol 14:479–493. https://doi.org/10.1038/nrmicro.2016.87.
8. Huang TS, Palese P, Krystal M. 1990. Determination of influenza virus proteins required for genome replication. J Virol 64:5669–5673.
9. Klumpp K, Ruigrok RW, Baudin F. 1997. Roles of the influenza virus polymerase and nucleoprotein in forming a functional RNP structure. EMBO J 16:1248–1257. https://doi.org/10.1093/emboj/16.6.1248.
10. Duesberg PH. 1969. Distinct subunits of the ribonucleoprotein of influenza virus. J Mol Biol 42:485–499. https://doi.org/10.1016/0022-2836(69)90237-X.
11. Hatta M, Gao P, Halfmann P, Kawaoka Y. 2001. Molecular basis for high virulence of Hong Kong H5N1 influenza A viruses. Science 293:1840–1842. https://doi.org/10.1126/science.1062882.
12. Pinto LH, Lamb RA. 2006. The M2 proton channels of influenza A and B viruses. J Biol Chem 281:8997–9000. https://doi.org/10.1074/jbc.R500020200.
13. Grantham ML, Stewart SM, Lalime EN, Pekosz A. 2010. Tyrosines in the influenza A virus M2 protein cytoplasmic tail are critical for production of infectious virus particles. J Virol 84:8765. https://doi.org/10.1128/JVI.00853-10.
14. Mccown MF, Pekosz A. 2006. Distinct domains of the influenza a virus M2 protein cytoplasmic tail mediate binding to the M1 protein and facilitate infectious virus production. J Virol 80:8178. https://doi.org/10.1128/JVI.00627-06.
15. McCown MF, Pekosz A. 2005. The influenza A virus M2 cytoplasmic tail is required for infectious virus production and efficient genome packaging. J Virol 79:3595–3605. https://doi.org/10.1128/JVI.79.6.3595-3605.2005.
16. Nayak DP, Balogun RA, Yamada H, Zhou ZH, Barman S. 2009. Influenza virus morphogenesis and budding. Virus Res 143:147–161. https://doi.org/10.1016/j.virusres.2009.05.010.
17. Rossman JS, Lamb RA. 2011. Influenza virus assembly and budding. Virology 411:229–236. https://doi.org/10.1016/j.virol.2010.12.003.
18. Mizushima N, Yoshimori T, Levine B. 2010. Methods in mammalian autophagy research. Cell 140:313–326. https://doi.org/10.1016/j.cell.2010.01.028.
19. Klionsky DJ, Emr SD. 2000. Autophagy as a regulated pathway of cellular degradation. Science 290:1717–1721. https://doi.org/10.1126/science.290.5497.1717.
20. Yang YP, Liang ZQ, Gu ZL, Qin ZH. 2005. Molecular mechanism and regulation of autophagy. Acta Pharmacol Sin 26:1421–1434. https://doi.org/10.1111/j.1745-7254.2005.00235.x.
21. Wang CW, Klionsky DJ. 2003. The molecular mechanism of autophagy. Mol Med 9:65–76. https://doi.org/10.1007/BF03402040.
22. Yang Z, Klionsky DJ. 2009. An overview of the molecular mechanism of autophagy. Curr Top Microbiol Immunol 335:1–32. https://doi.org/10.1007/978-3-642-00302-8_1.
23. Boya P, Reggiori F, Codogno P. 2013. Emerging regulation and functions of autophagy. Nat Cell Biol 15:713–720. https://doi.org/10.1038/ncb2788.
24. Yang Z, Klionsky DJ. 2010. Eaten alive: a history of macroautophagy. Nat Cell Biol 12:814. https://doi.org/10.1038/ncb0910-814.
25. Kroemer G, Marino G, Levine B. 2010. Autophagy and the integrated stress response. Mol Cell 40:280–293. https://doi.org/10.1016/j.molcel.2010.09.023.
26. Chan EY. 2009. mTORC1 phosphorylates the ULK1-mAtg13-FIP200 autophagy regulatory complex. Sci Signal 2:pe51. https://doi.org/10.1126/scisignal.284pe51.
27. Wong PM, Puente C, Ganley IG, Jiang X. 2013. The ULK1 complex: sensing nutrient signals for autophagy activation. Autophagy 9:124–137. https://doi.org/10.4161/auto.23323.
28. Nazarko VY, Zhong Q. 2013. ULK1 targets Beclin-1 in autophagy. Nat Cell Biol 15:727–728. https://doi.org/10.1038/ncb2797.
29. Ganley IG, Lam DH, Wang J, Ding X, Chen S, Jiang X. 2009. ULK1.ATG13.FIP200 complex mediates mTOR signaling and is essential for autophagy. J Biol Chem 284:12297–12305. https://doi.org/10.1074/jbc.M900573200.
30. Mercer CA, Kaliappan A, Dennis PB. 2009. A novel, human Atg13 binding protein, Atg101, interacts with ULK1 and is essential for macroautophagy. Autophagy 5:649–662. https://doi.org/10.4161/auto.5.5.8249.
31. Itakura E, Mizushima N. 2010. Characterization of autophagosome formation site by a hierarchical analysis of mammalian Atg proteins. Autophagy 6:764–776. https://doi.org/10.4161/auto.6.6.12709.
32. Xie Z, Klionsky DJ. 2007. Autophagosome formation: core machinery and adaptations. Nat Cell Biol 9:1102–1109. https://doi.org/10.1038/ncb1007-1102.
33. Rossman JS, Lamb RA. 2009. Autophagy, apoptosis, and the influenza virus M2 protein. Cell Host Microbe 6:299–300. https://doi.org/10.1016/j.chom.2009.09.009.
34. Romanov J, Walczak M, Ibiricu I, Schuchner S, Ogris E, Kraft C, Martens S. 2012. Mechanism and functions of membrane binding by the Atg5-Atg12/Atg16 complex during autophagosome formation. EMBO J 31:4304–4317. https://doi.org/10.1038/emboj.2012.278.
35. Nakatogawa H, Suzuki K, Kamada Y, Ohsumi Y. 2009. Dynamics and diversity in autophagy mechanisms: lessons from yeast. Nat Rev Mol Cell Biol 10:458–467. https://doi.org/10.1038/nrm2708.
36. Feng YC, Yao ZY, Klionsky DJ. 2015. How to control self-digestion: transcriptional, post-transcriptional, and post-translational regulation of autophagy. Trends Cell Biol 25:354–363. https://doi.org/10.1016/j.tcb.2015.02.002.
37. Huang R, Xu Y, Wan W, Shou X, Qian J, You Z, Liu B, Chang C, Zhou T, Lippincott-Schwartz J, Liu W. 2015. Deacetylation of nuclear LC3 drives autophagy initiation under starvation. Mol Cell 57:456–466. https://doi.org/10.1016/j.molcel.2014.12.013.
38. Huang R, Liu W. 2015. Identifying an essential role of nuclear LC3 for autophagy. Autophagy 11:852–853. https://doi.org/10.1080/15548627.2015.1038016.
39. Klionsky DJ, Abeliovich H, Agostinis P, Agrawal DK, Aliev G, Askew DS, Baba M, Baehrecke EH, Bahr BA, Ballabio A, Bamber BA, Bassham DC, Bergamini E, Bi XN, Biard-Piechaczyk M, Blum JS, Breclesen DE, Brodsky JL, Brumell JH, Brunk UT, Bursch W, Camougrand N, Cebollero E, Cecconi F, Chen YY, Chin LS, Choi A, Chu CT, Chung JK, Clarke PGH, Clark RSB, Clarke SG, Clave C, Cleveland JL, Codogno P, Colombo MI, Coto-Montes A, Cregg JM, Cuervo AM, Debnath J, Demarchi F, Dennis PB, Dennis PA, Deretic V, Devenish RJ, Di Sano F, Dice JF, DiFiglia M, Dinesh-Kumar S, Distelhorst CW, et al. 2008. Guidelines for the use and interpretation of assays for monitoring autophagy in higher eukaryotes. Autophagy 4:151–175. https://doi.org/10.4161/auto.5338.
40. Liang XH, Kleeman LK, Jiang HH, Gordon G, Goldman JE, Berry G, Herman B, Levine B. 1998. Protection against fatal Sindbis virus encephalitis by beclin, a novel Bcl-2-interacting protein. J Virol 72:8586–8596.
41. Liu Y, Schiff M, Czymmek K, Tallóczy Z, Levine B, Dinesh-Kumar SP. 2005. Autophagy regulates programmed cell death during the plant innate immune response. Cell 121:567–577. https://doi.org/10.1016/j.cell.2005.03.007.
42. Dreux M, Chisari FV. 2010. Viruses and the autophagy machinery. Cell Cycle 9:1295–1307. https://doi.org/10.4161/cc.9.7.11109.
43. Wong J, Zhang J, Si X, Gao G, Mao I, McManus BM, Luo H. 2008. Autophagosome supports coxsackievirus B3 replication in host cells. J Virol 82:9143–9153. https://doi.org/10.1128/JVI.00641-08.
44. Lee YR, Lei HY, Liu MT, Wang JR, Chen SH, Jiang-Shieh YF, Lin YS, Yeh TM, Liu CC, Liu HS. 2008. Autophagic machinery activated by dengue virus enhances virus replication. Virology 374:240–248. https://doi.org/10.1016/j.virol.2008.02.016.
45. Zhou Z, Jiang X, Liu D, Fan Z, Hu X, Yan J, Wang M, Gao GF. 2009. Autophagy is involved in influenza A virus replication. Autophagy 5:321–328. https://doi.org/10.4161/auto.5.3.7406.
46. Khakpoor A, Panyasrivanit M, Wikan N, Smith DR. 2009. A role for autophagolysosomes in dengue virus 3 production in HepG2 cells. J Gen Virol 90:1093–1103. https://doi.org/10.1099/vir.0.007914-0.
47. Ding B, Zhang G, Yang X, Zhang S, Chen L, Yan Q, Xu M, Banerjee AK, Chen M. 2014. Phosphoprotein of human parainfluenza virus type 3 blocks autophagosome-lysosome fusion to increase virus production. Cell Host Microbe 15:564–577. https://doi.org/10.1016/j.chom.2014.04.004.
48. Jackson WT, Giddings TH, Taylor MP, Mulinyawe S, Rabinovitch M, Kopito RR, Kirkegaard K. 2005. Subversion of cellular autophagosomal machinery by RNA viruses. PLoS Biol 3:e156. https://doi.org/10.1371/journal.pbio.0030156.
49. Prentice E, Jerome WG, Yoshimori T, Mizushima N, Denison MR. 2004. Coronavirus replication complex formation utilizes components of cellular autophagy. J Biol Chem 279:10136–10141. https://doi.org/10.1074/jbc.M306124200.
50. Tanida I, Fukasawa M, Ueno T, Kominami E, Wakita T, Hanada K. 2009.

Knockdown of autophagy-related gene decreases the production of infectious hepatitis C virus particles. Autophagy 5:937–945. https://doi.org/10.4161/auto.5.7.9243.
51. Guevin C, Manna DC, Konan KV, Mak P, Labonte P. 2010. Autophagy protein ATG5 interacts transiently with the hepatitis C virus RNA polymerase (NS5B) early during infection. Virology 405:1–7. https://doi.org/10.1016/j.virol.2010.05.032.
52. Shrivastava S, Raychoudhuri A, Steele R, Ray R, Ray RB. 2011. Knockdown of autophagy enhances the innate immune response in hepatitis C virus-infected hepatocytes. Hepatology 53:406–414. https://doi.org/10.1002/hep.24073.
53. Richards AL, Jackson WT. 2012. Intracellular vesicle acidification promotes maturation of infectious poliovirus particles. PLoS Pathog 8:e1003046. https://doi.org/10.1371/journal.ppat.1003046.
54. Dreux M, Gastaminza P, Wieland SF, Chisari FV. 2009. The autophagy machinery is required to initiate hepatitis C virus replication. Proc Natl Acad Sci U S A 106:14046–14051. https://doi.org/10.1073/pnas.0907344106.
55. Ku B, Woo J-S, Liang C, Lee K-H, Hong H-S, E X, Kim K-S, Jung JU, Oh B-H. 2008. Structural and biochemical bases for the inhibition of autophagy and apoptosis by viral BCL-2 of murine gamma-herpesvirus 68. PLoS Pathog 4:e25. https://doi.org/10.1371/journal.ppat.0040025.
56. Taylor MP, Kirkegaard K. 2008. Potential subversion of autophagosomal pathway by picornaviruses. Autophagy 4:286–289. https://doi.org/10.4161/auto.5377.
57. Zhu B, Zhou Y, Xu F, Shuai J, Li X, Fang W. 2012. Porcine circovirus type 2 induces autophagy via the AMPK/ERK/TSC2/mTOR signaling pathway in PK-15 cells. J Virol 86:12003–12012. https://doi.org/10.1128/JVI.01434-12.
58. Sun P, Zhang SM, Qin XD, Chang XN, Cui XR, Li HT, Zhang SJ, Gao HH, Wang PH, Zhang ZD, Luo JX, Li ZY. 2018. Foot-and-mouth disease virus capsid protein VP2 activates the cellular EIF2S1-ATF4 pathway and induces autophagy via HSPB1. Autophagy 14:336–346. https://doi.org/10.1080/15548627.2017.1405187.
59. Orvedahl A, MacPherson S, Sumpter R, Talloczy Z, Zou ZJ, Levine B. 2010. Autophagy protects against Sindbis virus infection of the central nervous system. Cell Host Microbe 7:115–127. https://doi.org/10.1016/j.chom.2010.01.007.
60. Hu B, Zhang Y, Jia L, Wu H, Fan C, Sun Y, Ye C, Liao M, Zhou J. 2015. Binding of the pathogen receptor HSP90AA1 to avibirnavirus VP2 induces autophagy by inactivating the AKT-MTOR pathway. Autophagy 11:503–515. https://doi.org/10.1080/15548627.2015.1017184.
61. Sun Y, Li C, Shu Y, Ju X, Zou Z, Wang H, Rao S, Guo F, Liu H, Nan W, Zhao Y, Yan Y, Tang J, Zhao C, Yang P, Liu K, Wang S, Lu H, Li X, Tan L, Gao R, Song J, Gao X, Tian X, Qin Y, Xu KF, Li D, Jin N, Jiang C. 2012. Inhibition of autophagy ameliorates acute lung injury caused by avian influenza A H5N1 infection. Sci Signal 5:ra16.
62. Gannagé M, Dormann D, Albrecht R, Dengjel J, Torossi T, Rämer PC, Lee M, Strowig T, Arrey F, Conenello G, Pypaert M, Andersen J, García-Sastre A, Münz C. 2009. Matrix protein 2 of influenza A virus blocks autophagosome fusion with lysosomes. Cell Host Microbe 6:367–380. https://doi.org/10.1016/j.chom.2009.09.005.
63. Zhirnov OP, Klenk HD. 2013. Influenza A virus proteins NS1 and hemagglutinin along with M2 are involved in stimulation of autophagy in infected cells. J Virol 87:13107–13114. https://doi.org/10.1128/JVI.02148-13.
64. Seglen PO, Gordon PB. 1982. 3-Methyladenine: specific inhibitor of autophagic/lysosomal protein degradation in isolated rat hepatocytes. Proc Natl Acad Sci U S A 79:1889–1892. https://doi.org/10.1073/pnas.79.6.1889.
65. Eierhoff T, Ludwig S, Ehrhardt C. 2009. The influenza A virus matrix protein as a marker to monitor initial virus internalisation. Biol Chem 390:509–515. https://doi.org/10.1515/BC.2009.053.
66. Liu G, Zhong M, Guo C, Komatsu M, Xu J, Wang Y, Kitazato K. 2016. Autophagy is involved in regulating influenza A virus RNA and protein synthesis associated with both modulation of Hsp90 induction and mTOR/p70S6K signaling pathway. Int J Biochem Cell B 72:100–108. https://doi.org/10.1016/j.biocel.2016.01.012.
67. Momose F, Naito T, Yano K, Sugimoto S, Morikawa Y, Nagata K. 2002. Identification of Hsp90 as a stimulatory host factor involved in influenza virus RNA synthesis. J Biol Chem 277:45306–45314. https://doi.org/10.1074/jbc.M206822200.
68. Naito T, Momose F, Kawaguchi A, Nagata K. 2007. Involvement of Hsp90 in assembly and nuclear import of influenza virus RNA polymerase subunits. J Virol 81:1339–1349. https://doi.org/10.1128/JVI.01917-06.
69. Sato S, Fujita N, Tsuruo T. 2000. Modulation of Akt kinase activity by binding to Hsp90. Proc Natl Acad Sci U S A 97:10832–10837. https://doi.org/10.1073/pnas.170276797.
70. Makhnevych T, Houry WA. 2012. The role of Hsp90 in protein complex assembly. Biochim Biophys Acta 1823:674–682. https://doi.org/10.1016/j.bbamcr.2011.09.001.
71. Ehrhardt C, Marjuki H, Wolff T, Nurnberg B, Planz O, Pleschka S, Ludwig S. 2006. Bivalent role of the phosphatidylinositol-3-kinase (PI3K) during influenza virus infection and host cell defence. Cell Microbiol 8:1336–1348. https://doi.org/10.1111/j.1462-5822.2006.00713.x.
72. Shin YK, Liu Q, Tikoo SK, Babiuk LA, Zhou Y. 2007. Effect of the phosphatidylinositol 3-kinase/Akt pathway on influenza A virus propagation. J Gen Virol 88:942–950. https://doi.org/10.1099/vir.0.82483-0.
73. Kirkegaard K. 2009. Subversion of the cellular autophagy pathway by viruses. Curr Top Microbiol Immunol 335:323–333. https://doi.org/10.1007/978-3-642-00302-8_16.
74. Crawford SE, Hyser JM, Utama B, Estes MK. 2012. Autophagy hijacked through viroporin-activated calcium/calmodulin-dependent kinase kinase-β signaling is required for rotavirus replication. Proc Natl Acad Sci U S A 109:20175–20175.
75. Momose F, Basler CF, O'Neill RE, Iwamatsu A, Palese P, Nagata K. 2001. Cellular splicing factor RAF-2p48/NPI-5/BAT1/UAP56 interacts with the influenza virus nucleoprotein and enhances viral RNA synthesis. J of Virology 75:1899–1908. https://doi.org/10.1128/JVI.75.4.1899-1908.2001.
76. Reed LJ, Muench H. 1938. A simple method of estimating fifty percent endpoints. Am J Epidemiol 27:493–497. https://doi.org/10.1093/oxfordjournals.aje.a118408.